Sensitive broadband binary photoresponsivity in 4H-SiC epitaxial graphene

Dinesh Kumar Patel [1, 2, 3], Shivi Rathore [4], Mukesh Kumar Thakur [5], Golam Haider [5], Martin Kalbac [5], Mattias Kruskopf [3], Chieh-I Liu [6], Albert F. Rigosi [2], Randolph E. Elmquist [2], Chi-Te Liang [1], Po-Da Hong [4]

[1] *Department of Physics, National Taiwan University, Taipei, 106319, Taiwan*

[2] *Physical Measurement Laboratory, National Institute of Standards and Technology (NIST), Gaithersburg, MD, 20899, USA*

[3] *Physikalisch-Technische Bundesanstalt (PTB), Bundesallee 100, D-38116, Braunschweig, Germany*

[4] *Department of Materials Science and Engineering, National Taiwan University of Science and Technology, Taipei, 106335, Taiwan*

[5] *J. Heyrovsky Institute of Physical Chemistry, Czech Academy of Sciences, Prague 8, Czech Republic*

[6] *Department of Chemistry and Biochemistry, University of Maryland, College Park, MD, 20742, USA*

Abstract: Due to weak light-matter interaction, standard chemical vapor deposition (CVD)/exfoliated single-layer graphene-based photodetectors show low photoresponsivity (on the order of mA/W). However, epitaxial graphene (EG) offers a more viable approach for obtaining devices with good photoresponsivity. EG on 4H–SiC also hosts an interfacial buffer layer (IBL), which is the source of electron carriers applicable to quantum optoelectronic devices. We utilize these properties to demonstrate a gate-free, planar EG/4H–SiC-based device that enables us to observe the positive photoresponse for (405 to 532) nm and negative photoresponse for (632–980) nm laser excitation. The broadband binary photoresponse mainly originates from the energy band alignment of the IBL/EG interface and the highly sensitive work function of the EG. We find that the photoresponsivity of the device is > 10 A/W under 405 nm of power density 7.96 mW/cm^2 at 1 V applied bias, which is three orders of magnitude greater than the obtained values of exfoliated graphene, as well as graphene obtained by chemical vapor deposition (CVD), and higher than the required value for practical applications. These results path the way for selective light-triggered logic devices based on EG and can open a new window for broadband photodetection.

Introduction

Recently, graphene has attracted much attention in the area of optoelectronic devices due to its high carrier mobility, optical transparency, mechanical flexibility, strength, and thermal stability [1-2]. Exhibited ultrafast and broadband absorption makes graphene an ideal candidate for broadband photodetectors [3, 4]. Designing a binary photoresponse device based on graphene alone would be highly beneficial for optical signal processing and logic device applications [5]. However, pristine exfoliated and chemical vapor deposited (CVD) monolayer graphene yield photodetector devices that suffer from low-photocurrent responsivity [6]. Therefore, developing a better performing, graphene-based binary photodetector is highly desired. Solid-state and wideband gap-based silicon carbide (SiC) and GaN-based photodetectors are popular due to their reliability and light weight. Specifically, epitaxial graphene (EG) on SiC could be a better choice for these practical electronic applications due to its high breakdown fields, inherent bandgap induced by the underpinning interfacial buffer layer (IBL), and its metrology-grade quality [7-13].

In this work, we demonstrate, for the first time, electrostatic gate-free, broadband, and binary photoresponses in EG/4H-SiC-based devices having the simplest device design. We use as grown bare monolayer EG on 4H-SiC substrate to fabricate devices. We report both positive and negative photoresponse observations without the assistance of electrostatic gating under the illumination of the different wavelengths of laser light. Additionally, our devices responded strongly to excitation wavelengths ranging from 405 nm to 980 nm, yielding unprecedented responsivities higher than 10 A/W under 405 nm of power 7.96 mW/cm^2, which is three orders of magnitude higher than the CVD and exfoliated graphene. This unusual phenomenon motivates us to study the photodetection in such devices as well as to test the significance of the IBL in the photodetection process. Further confirmation of the photodetection mechanism is provided by carefully studying two different control devices without the IBL on the similar SiC substrate: (1) a thin layer of exfoliated graphene with pre-fabricated electrodes on only bare SiC to see the effects of the IBL and metal contacts, (2) a dummy device with two electrodes on only SiC to understand the role of the substrate.

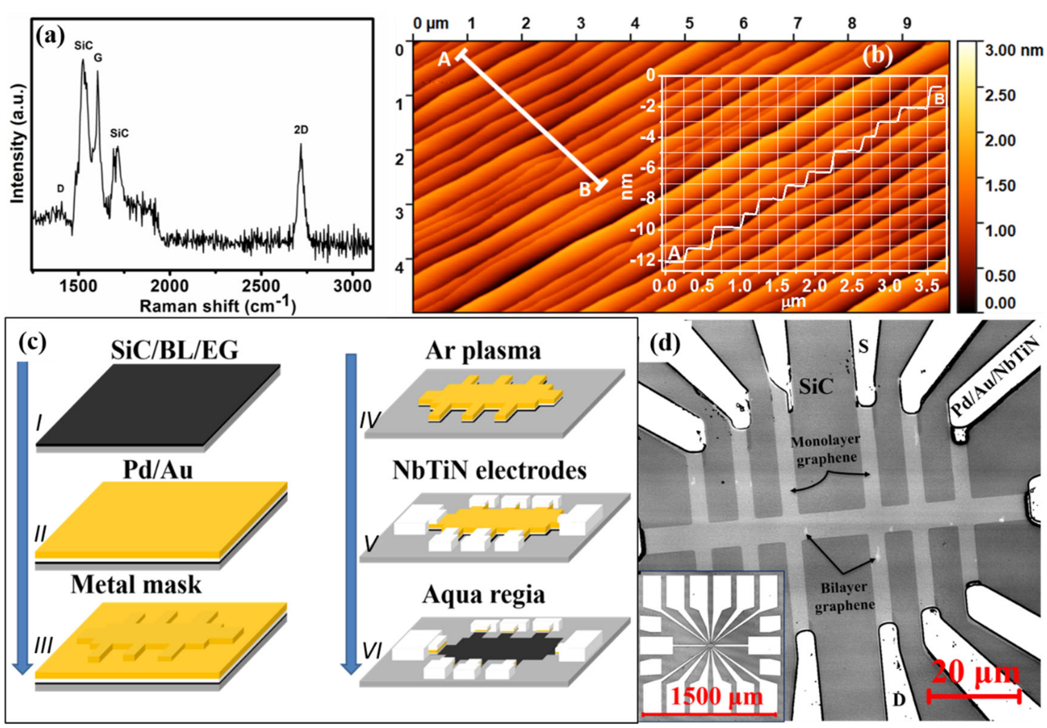

Fig. 1. Fabrication and optical characterization of the device. (a) Raman spectrum of the EG/4H-SiC showing 2D, G and D peak around 2716.6 ± 0.8 cm^{-1}, 1604.5 ± 0.6 cm^{-1} and 1384.5 ± 8.9 cm^{-1}

respectively including SiC peaks around 1524 cm^{-1} and 1718 cm^{-1}. (b) The AFM image shows the uniform surface morpholgy of the EG on the SiC substrate. The inset shows the height profile with typical terrace step heights of about 1 nm. (c) Schematic of the residue-free device fabrication process. After the EG growth on SiC, a thin layer of palladium and gold is deposited to protect the film. Photolithography and sputtering were then used to complete the device. Finally, the protective metals are etched from EG with diluted aqua regia. (d) The confocal microscopy image of the EG/4H-SiC-based device is shown. The image highlights the homogeneity of the EG film, showing a few small patches containing bilayers, as indicated by arrow. Inset is the confocal image of a complete device in which fourteen NbTiN electrodes are connected to the EG.

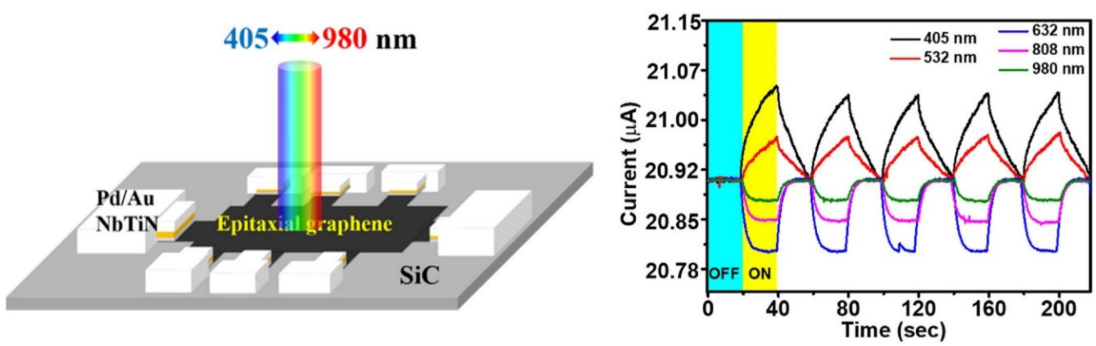

Fig. 2. (left) Schematic illustration of the EG/4H-SiC-based device and two-probe photodetector measurement setup with IBL under EG. (right) Dynamic photoresponse of the EG/4H-SiC-based device under 405 nm, 532 nm, 632 nm, 808 nm, and 980 nm excitation of intensity 79.6 mW/cm^2 at V_{DS} = 1V. The switching behaviour of the device is marked as ON, and OFF in the first cycle.

Acknowledgements:

The authors would like to express thanks to S Mhatre and A Levy for their assistance in the NIST internal review process.

Commercial equipment, instruments, and materials are identified in this paper in order to specify the experimental procedure adequately. Such identification is not intended to imply recommendation or endorsement by the National Institute of Standards and Technology or the United States government, nor is it intended to imply that the materials or equipment identified are necessarily the best available for the purpose.

References

[1] Thakur, M.K., Gupta, A., Ghosh, S. and Chattopadhyay, S., 2019. Graphene-conjugated upconversion nanoparticles as fluorescence-tuned photothermal nanoheaters for desalination. *ACS Applied Nano Materials*, *2*(4), pp.2250-2259.

[2] Novoselov, K.S., Colombo, L., Gellert, P.R., Schwab, M.G. and Kim, K., 2012. A roadmap for graphene. *nature*, *490*(7419), pp.192-200.

[3] Nair, R.R., Blake, P., Grigorenko, A.N., Novoselov, K.S., Booth, T.J., Stauber, T., Peres, N.M. and Geim, A.K., 2008. Fine structure constant defines visual transparency of graphene. *Science*, *320*(5881), pp.1308-1308.

[4] Koppens, F.H.L., Mueller, T., Avouris, P., Ferrari, A.C., Vitiello, M.S. and Polini, M., 2014. Photodetectors based on graphene, other two-dimensional materials and hybrid systems. *Nature nanotechnology*, *9*(10), pp.780-793.

[5] Chen, J., Xu, J., Shi, S., Cao, R., Liu, D., Bu, Y., Yang, P., Xu, J., Zhang, X. and Li, L., 2020. Novel Self-Powered Photodetector with Binary Photoswitching Based on SnS x/TiO2 Heterojunctions. *ACS Applied Materials & Interfaces*, *12*(20), pp.23145-23154.

[6] Yan, K., Wu, D., Peng, H., Jin, L., Fu, Q., Bao, X. and Liu, Z., 2012. Modulation-doped growth of mosaic graphene with single-crystalline p–n junctions for efficient photocurrent generation. *Nature communications*, *3*(1), pp.1-7.

[7] Patel, D., Marzano, M., Liu, C.I., Hill, H.M., Kruskopf, M., Jin, H., Hu, J., Newell, D.B., Liang, C.T., Elmquist, R. and Rigosi, A.F., 2020. Accessing ratios of quantized resistances in graphene p–n junction devices using multiple terminals. *AIP Advances*, *10*(2), p.025112.

[8] Panna, A.R., Hu, I.F., Kruskopf, M., Patel, D.K., Jarrett, D.G., Liu, C.I., Payagala, S.U., Saha, D., Rigosi, A.F., Newell, D.B. and Liang, C.T., 2021. Graphene quantum Hall effect parallel resistance arrays. *Physical Review B*, *103*(7), p.075408.

[9] Rigosi, A.F., Marzano, M., Levy, A., Hill, H.M., Patel, D.K., Kruskopf, M., Jin, H., Elmquist, R.E. and Newell, D.B., 2020. Analytical determination of atypical quantized resistances in graphene pn junctions. *Physica B: Condensed Matter*, *582*, p.411971.

[10] Oe, T., Rigosi, A.F., Kruskopf, M., Wu, B.Y., Lee, H.Y., Yang, Y., Elmquist, R.E., Kaneko, N.H. and Jarrett, D.G., 2019. Comparison between NIST graphene and AIST GaAs quantized Hall devices. *IEEE transactions on instrumentation and measurement*, *69*(6), pp.3103-3108.

[11] Hu, J., Rigosi, A.F., Lee, J.U., Lee, H.Y., Yang, Y., Liu, C.I., Elmquist, R.E. and Newell, D.B., 2018. Quantum transport in graphene p− n junctions with moiré superlattice modulation. *Physical Review B*, *98*(4), p.045412.

[12] Hill, H.M., Rigosi, A.F., Chowdhury, S., Yang, Y., Nguyen, N.V., Tavazza, F., Elmquist, R.E., Newell, D.B. and Walker, A.R.H., 2017. Probing the dielectric response of the interfacial buffer layer in epitaxial graphene via optical spectroscopy. *Physical Review B*, *96*(19), p.195437.

[13] Rigosi, A.F., Hill, H.M., Glavin, N.R., Pookpanratana, S.J., Yang, Y., Boosalis, A.G., Hu, J., Rice, A., Allerman, A.A., Nguyen, N.V. and Hacker, C.A., 2017. Measuring the dielectric and optical response of millimeter-scale amorphous and hexagonal boron nitride films grown on epitaxial graphene. *2D Materials*, *5*(1), p.011011.